``Enseigner la recherche en train de se faire"

COLLÈGE DE FRANCE
1530

Chaire de
Physique de la Matière Condensée

CORRELATIONS ELECTRONIQUES ET TRANSPORT DANS LES OXYDES 4d ET COMPOSES SUPRACONDUCTEURS DU FER : HUND PLUTOT QUE MOTT, DRUDE PLUTOT QUE LANDAU

Les mercredis dans l'amphithéâtre Maurice Halbwachs
11, place Marcelin Berthelot 75005 Paris
Cours à 14h30 - Séminaire à 15h45

Antoine Georges

Cycle 2011-2012
2/05/2012 – 13/06/2012
(Pas de séance le 23/05)

Séance du 16 mai 2012

- **Cours à 14h30 –**

Etat métallique des ruthenates et composés supraconducteurs du fer: rôle du couplage de Hund.

- **Séminaire : 15h45 –**

Silke BIERMANN, CPHT *Ecole Polytechnique*

Hubbard and Hund: Dynamical Screening Effects in Iron Pnictide Compounds from First Principles

- ***Séminaire: 16h45***

Luca de' Medici, LPS Orsay

Orbital-Selective Mott Transitions and their relevance to Fe-superconductors

Pas de séance le 23 mai

Reprise le 30 mai (Transport)

Séminaires du 30 mai: F. Rullier-Albenque, N. Barisic

Recall: a model study: 3 degenerate bands w/ same bandwidth 2D

occupied by N electrons per site

$$H_{\rm int} = U \sum_m n_{m\uparrow} n_{m\downarrow} +$$
$$+ \sum_{m<n,\sigma} [(U-2J) n_{m\sigma} n_{n\sigma} + (U-3J) n_{m\sigma} n_{n\sigma}]$$
$$- J \sum_{m<n} [d^\dagger_{m\uparrow} d_{m\downarrow} d^\dagger_{n\downarrow} d_{n\uparrow} + d^\dagger_{m\uparrow} d^\dagger_{m\downarrow} d_{n\uparrow} d_{n\downarrow} + \text{h.c.}]$$
$$= (U-3J) \frac{\hat{N}(\hat{N}-1)}{2} + \frac{5}{2} J \hat{N} - 2J \vec{S}^2 - \frac{1}{2} J \vec{T}^2$$

P.Werner et al. PRL 101 (2008) 166405
L de'Medici, J.Mravlje, AG PRL 107 (2011) 256401

studied with : DMFT

Dependence of Mott U_c on J, in hindsight

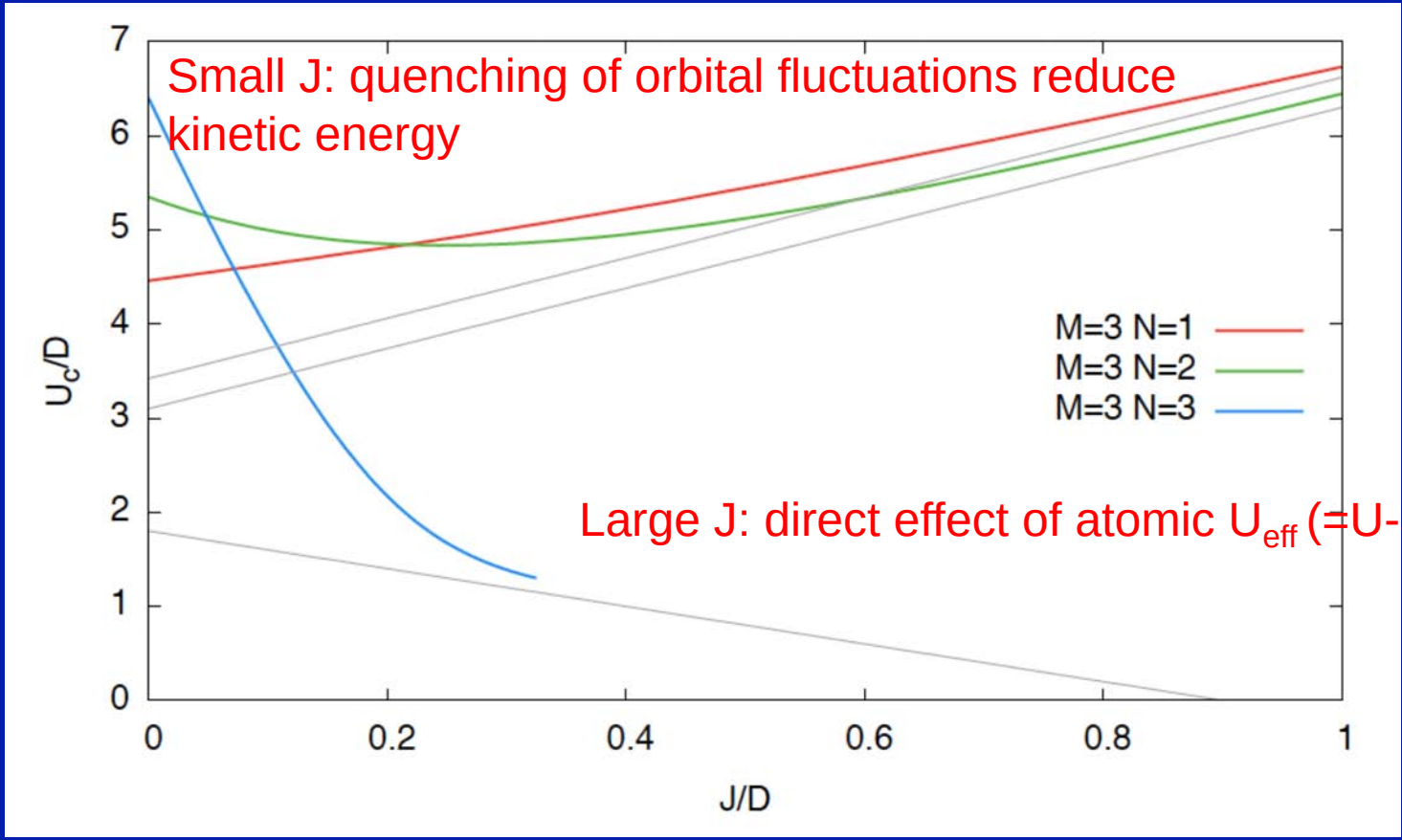

Figure 1: Critical coupling separating the metallic and Mott insulating (paramagnetic) phase, as a function of the Hund's rule coupling, for a Hubbard-Kanamori model of three degenerate bands with one (red), two (green) and three (blue) electrons per site. The model is solved with DMFT, with a semi-circular density of states of bandwidth $2D$ for each band. See Refs. [20, 27].

Key points

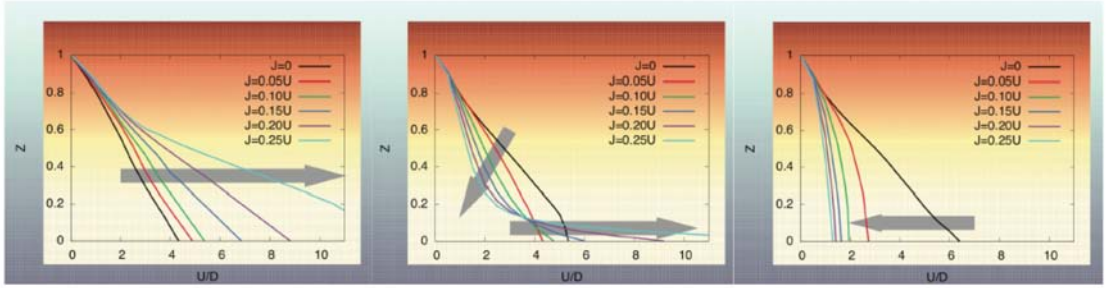

(a) $N = 1$ (b) $N = 2$ (c) $N = 3$

Figure 1: Quasiparticle weight Z *vs.* U for $N = 1, 2, 3$ electrons in $M = 3$ orbitals. The grey arrows indicate the influence of an increasing Hund's rule coupling J/U.

* At ½ filling (3 el. In 3 orbitals) Mott critical U_c is strongly reduced upon increasing J

cf. Bunemann, Weber, Gebhard et al.; Han, Jarrell, Cox PRB1998

- IN CONTRAST, away from ½ filling (e.g. N=1,2,4,5) U_c is strongly ENHANCED

cf. L. de' Medici PRB 83, 205112 (2011)

- At the same time, quasiparticle coherence scale (~ZD) is strongly SUPPRESSED as J is increased cf. Suppression of Kondo scale

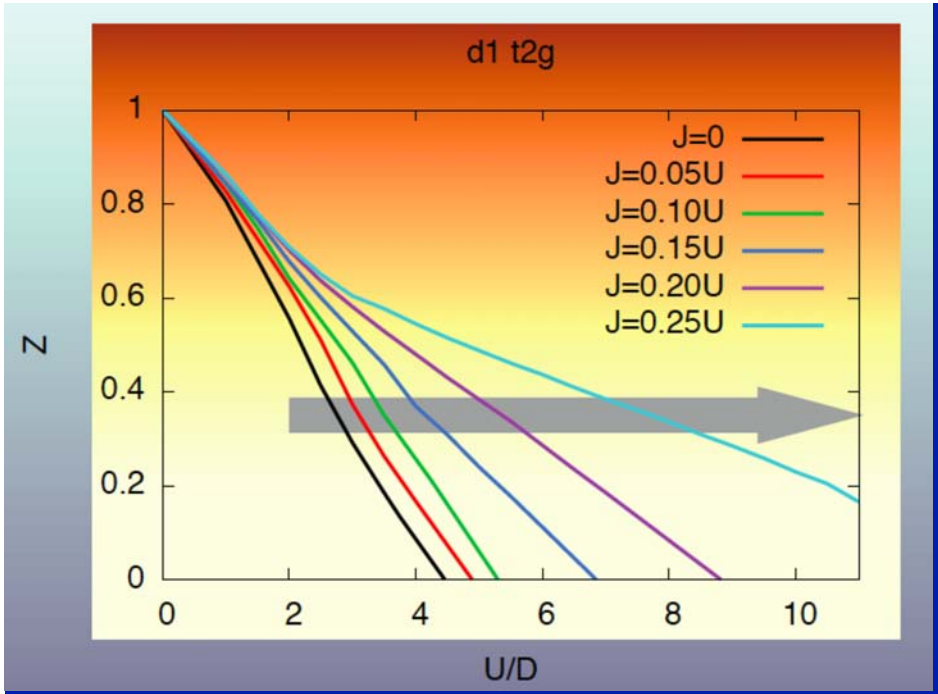

N=1 electron

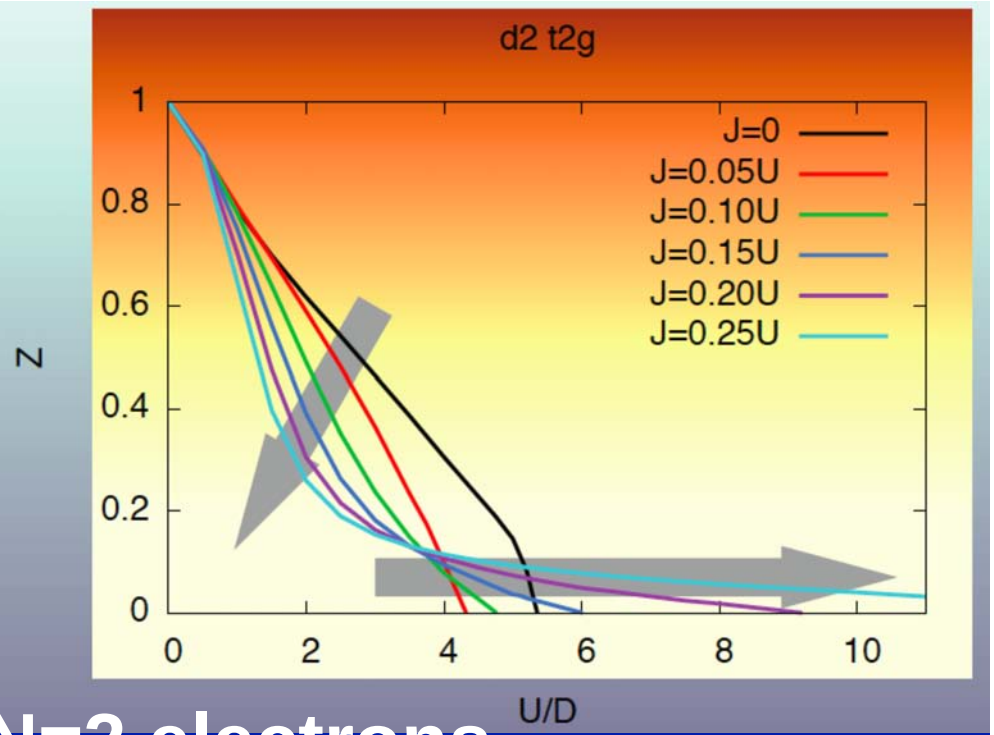

N=2 electrons

Quasiparticle weight Z vs. U/D

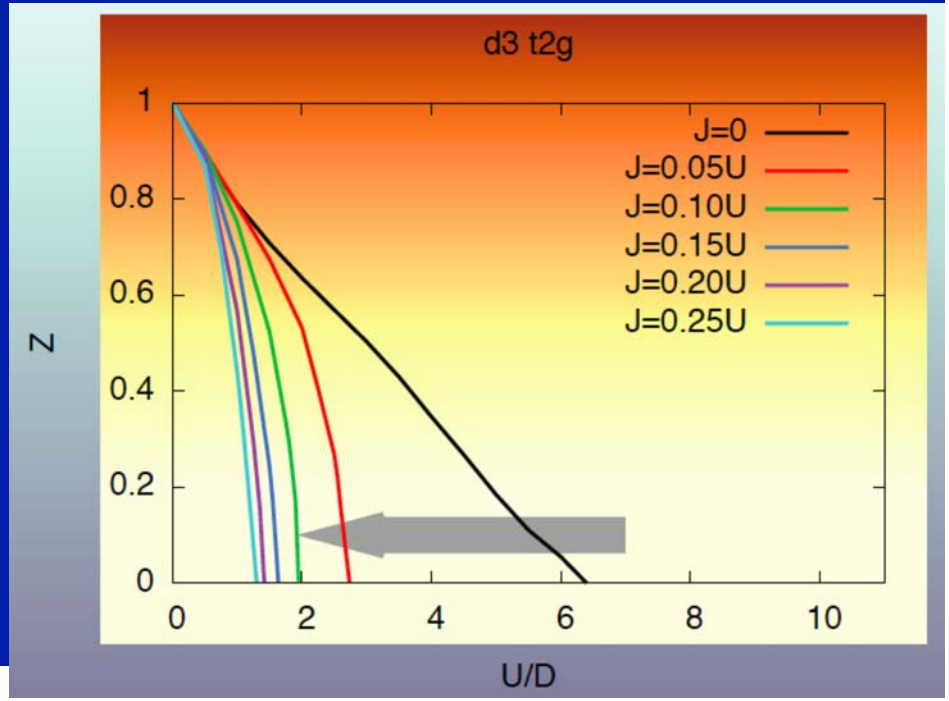

N=3 electrons

For N=2,4: Hund suppresses coherence scale →
« Bad metal » behaviour, small Z

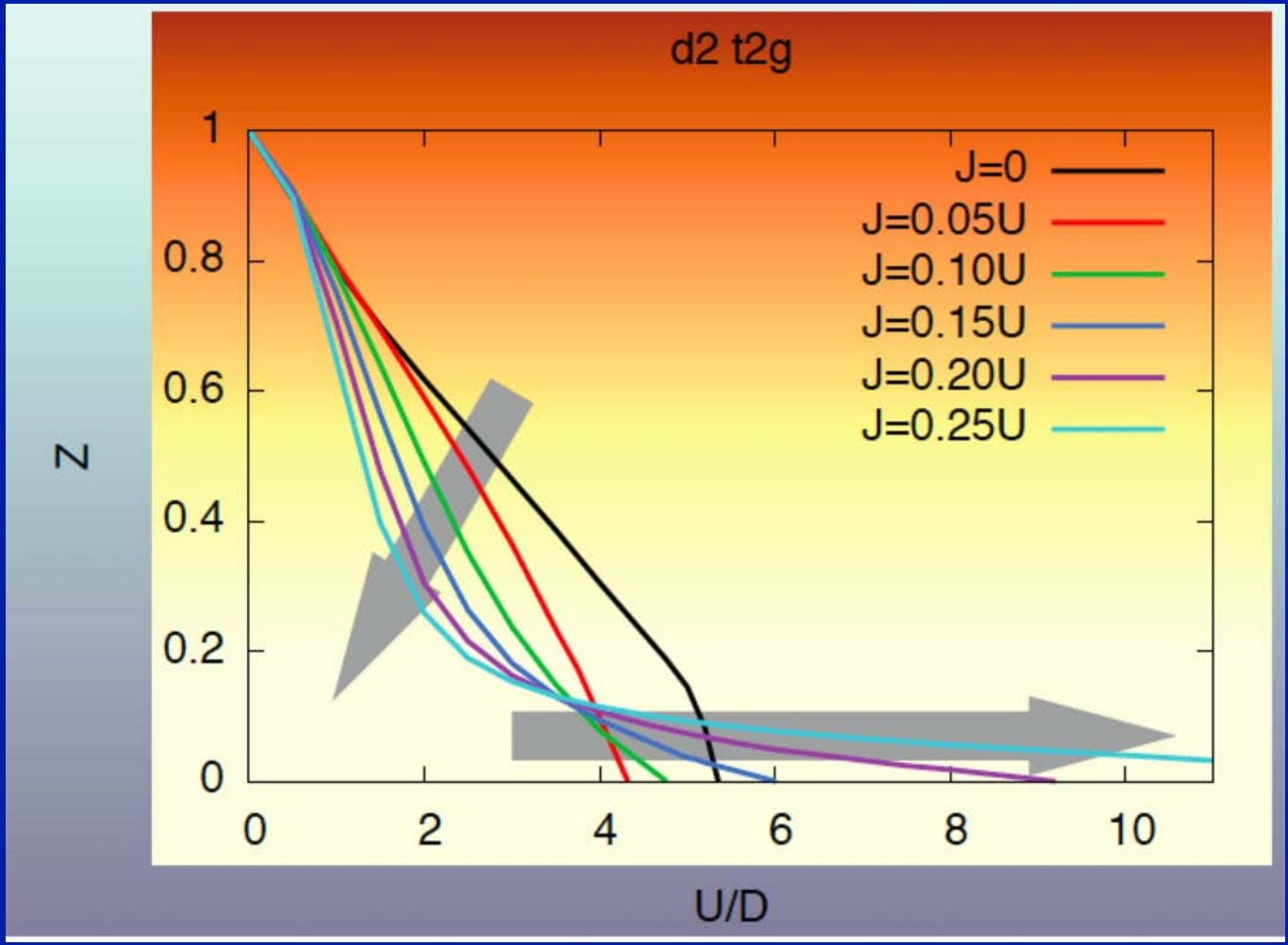

Increases U_c → Enhances range of metallic state

As a result, for generic filling…

(i.e. not ½ filling
and not 1 electron or hole)
e.g. for 2 or 4 electrons
in degenerate t_{2g} bands

… J is « Janus-faced » :
it has two ANTAGONISTIC effects

Janus is the latin god of beginnings/ transitions and is often associated with doors and entrances and has two faces.
His first mention in physics is due to P.G. de Gennes

Drawing a map of early transition-metal oxides (both 3d and 4d) with Hund's rule coupling as guidance

Cf. ``Atsushi Fujimori's map of RMO_3 perovskites''

J.Phys Chem Sol. 53 (1992) 1595

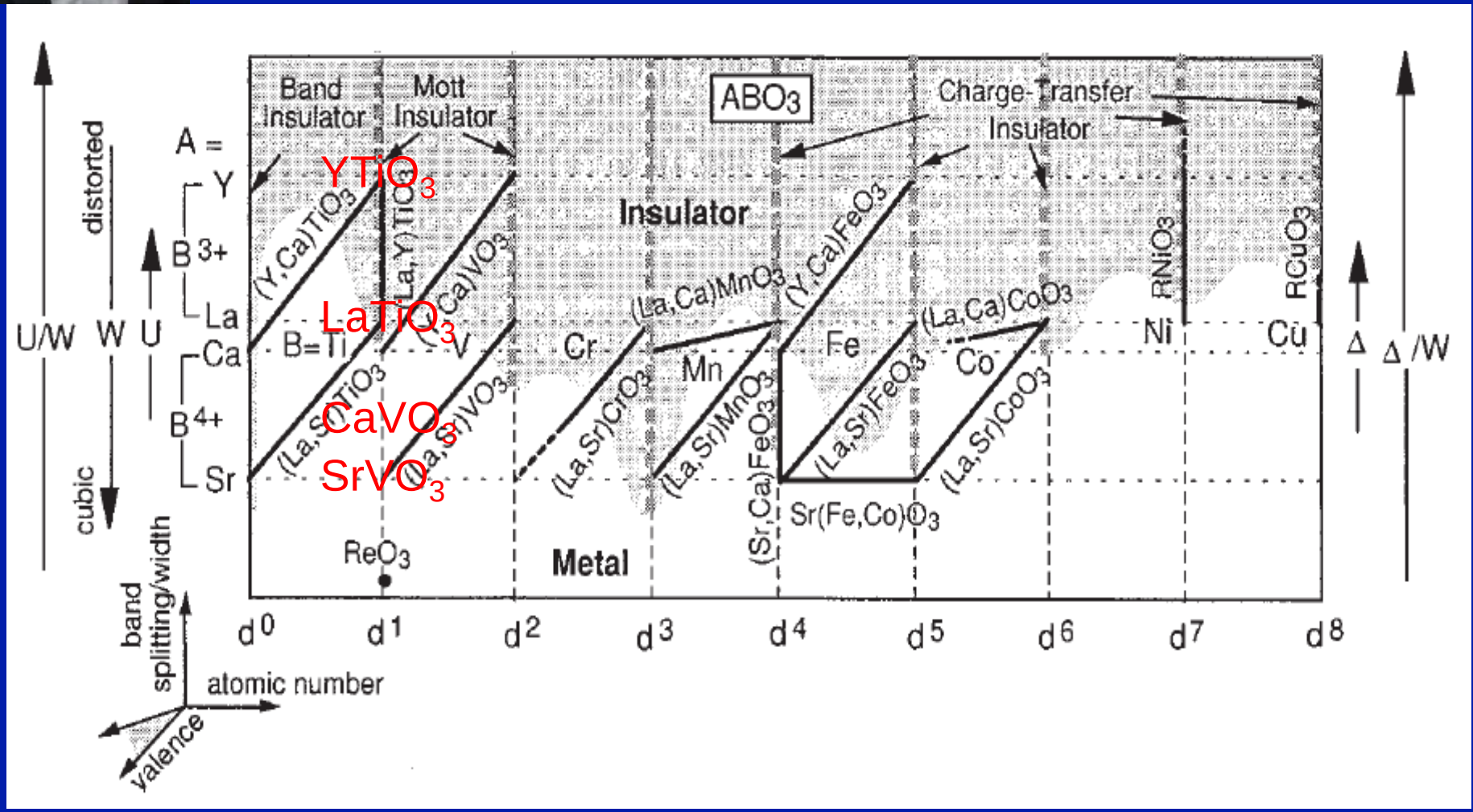

Partially filled d-shells… and yet often insulators

Correlation effects in 4d oxides due to J, not to Mott physics (except when strong splitting between orbitals)

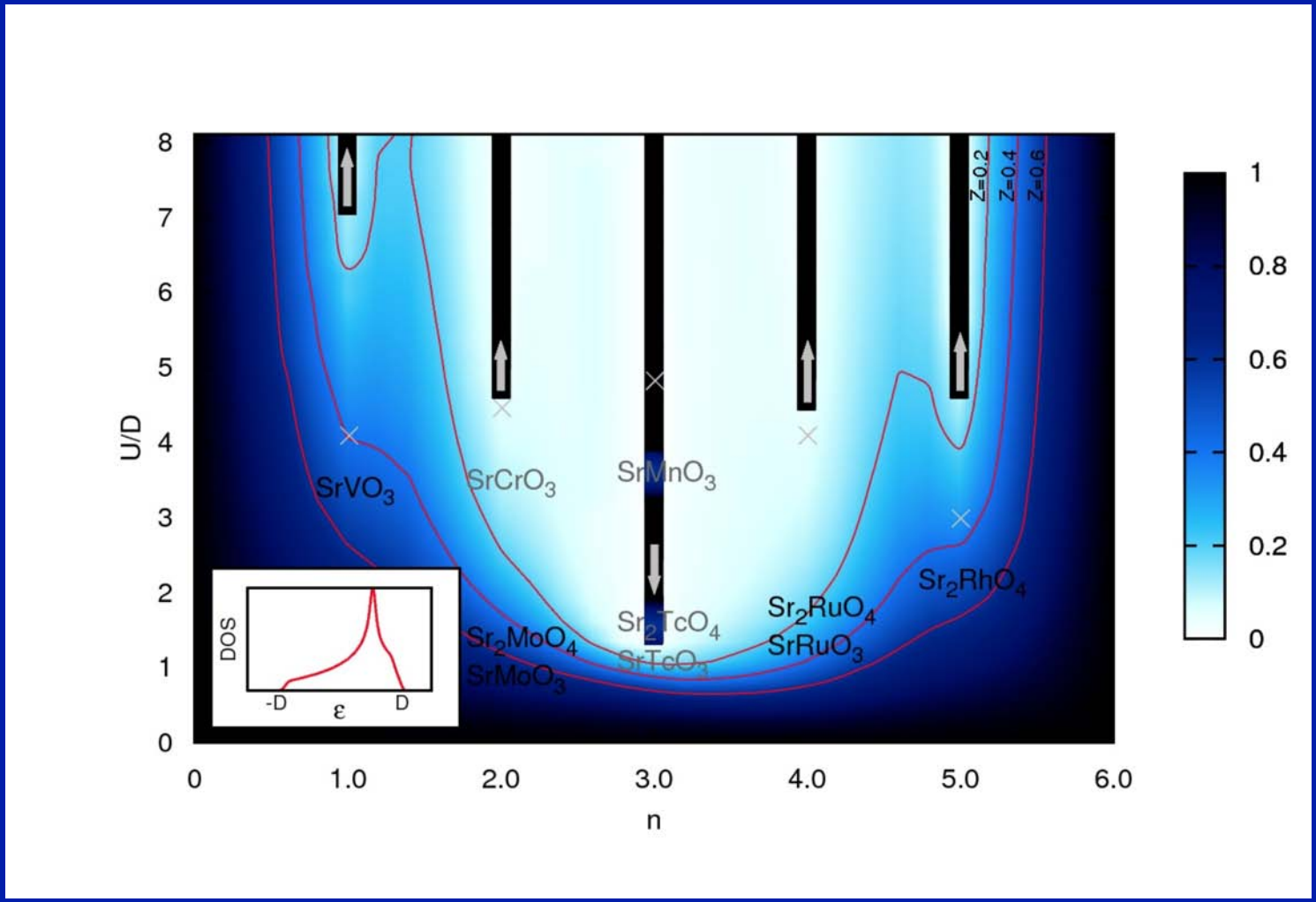

3d oxides: U/D ~ 4
4d oxides: U/D ~ 2

Focus in the following on:
Technetium and Ruthenate oxides

OUTLINE of this lecture:

- 1. A remark on AF order in Technetium
- 2. Evidence for key role of Hund's coupling in ruthenate Sr_2RuO_4
- 3. Nature of the `spin-freezing' non-Fermi liquid regime:

- Behaviour of physical quantities and possible relevance
- Status of theoretical understanding

4. Moving on to iron pnictides and chalcogenides

→ seminars

1. Record-high Néel temperature in Technetium oxide ($SrTcO_3$) - contrast to $SrMnO_3$

PRL **106,** 067201 (2011) PHYSICAL REVIEW LETTERS week ending 11 FEBRUARY 2011

High Temperature Magnetic Ordering in the 4*d* Perovskite $SrTcO_3$

Efrain E. Rodriguez,[1] Frédéric Poineau,[2] Anna Llobet,[3] Brendan J. Kennedy,[4] Maxim Avdeev,[5] Gordon J. Thorogood,[6] Melody L. Carter,[6] Ram Seshadri,[7] David J. Singh,[8] and Anthony K. Cheetham[9]

We present evidence for possibly the highest magnetic ordering temperature in any compound without 3*d* transition elements. Neutron powder diffraction measurements, at both time-of-flight and constant wavelength sources, were performed on two independently prepared $SrTcO_3$ powders. $SrTcO_3$ adopts a distorted perovskite structure with *G*-type antiferromagnetic ordering and has a moment of $1.87(4)\mu_B$ per Tc cation at room temperature with an extraordinarily high Néel point close to 750 °C. Electronic structure calculations reveal extensive mixing between the technetium 4*d* states and oxygen states proximal to the Fermi level. This hybridization leads to a close relationship between magnetic ordering temperature and moment formation in $SrTcO_3$.

Mechanism: $SrTcO_3$ (T_N~1000K) very close to Mott transition (Hund lowers U_c)

(In contrast $SrMnO_3$ is a more localized insulator, T_N ~ 260 K)

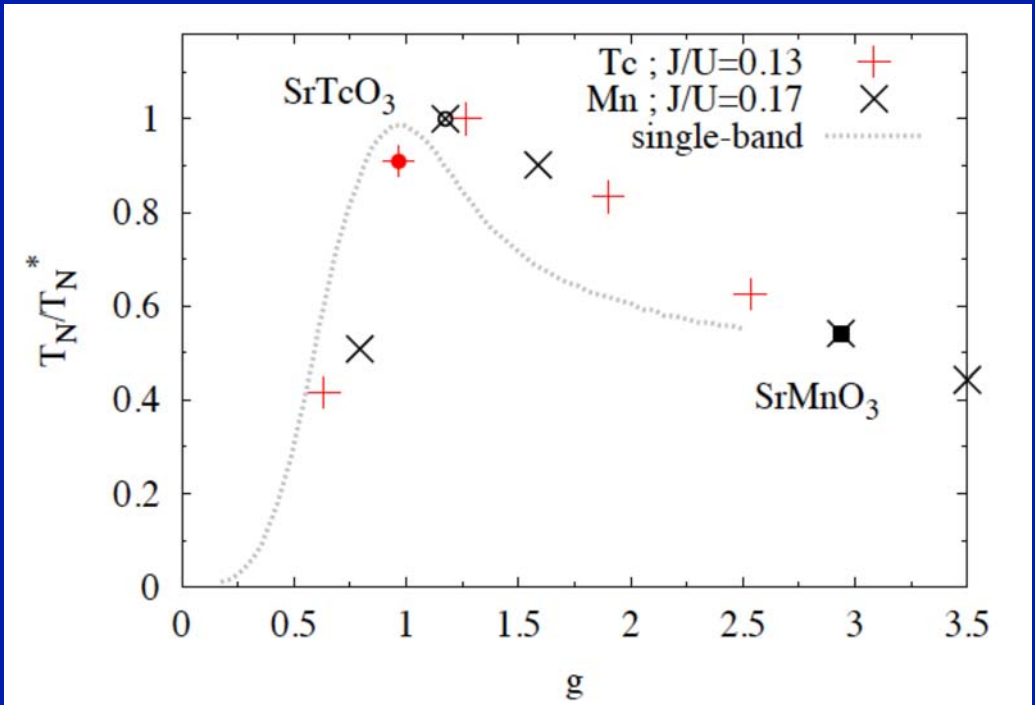

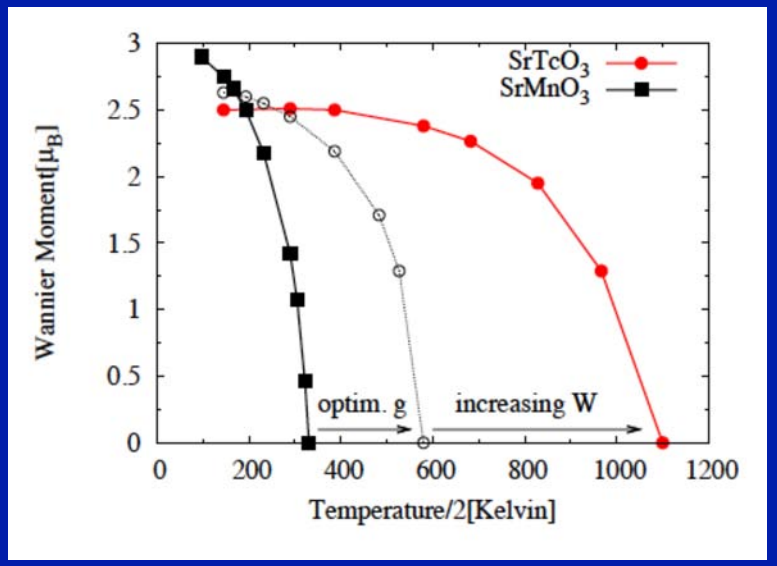

J.Mravlje et al.
PRL 108,
197202 (2012)

Figure 3. The Néel temperatures as a function of coupling $g \equiv \mathcal{U}/\mathcal{U}_c$, with $\mathcal{U} \equiv U + 2J$ and $\mathcal{U}_c = (U + 2J)_c$ the value at which the metal-insulator transition occurs in the paramagnetic state. T_N are normalized to the maximum Néel temperature T_N^* found when varying $\mathcal{U}$. The gray line is for the single-band Hubbard model (DMFT calculation of Ref. [19]).

2. Sr_2RuO_4: A Hund's correlated metal

J.Mravlje et al., PRL 106, 096401 (2011)

Ruthenates: cf. seminar last week by F.Baumberger

Sr_2RuO_4: the `Helium 3' of transition-metal oxides !

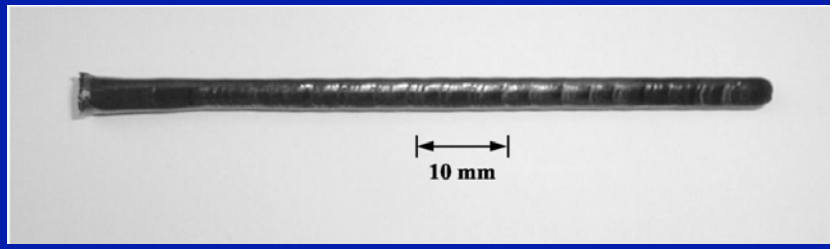

- Huge high-quality crystals !
- Has been investigated with basically all techniques in the experimentalist's toolbox
- 4d-row structural analogue of La_2CuO_4
- Beautiful review articles:

- A.Mackenzie and Y.Maeno

  RMP 75, 657 (2003)
- Bergemann, Adv. Phys. 52, 639 (2003)

  [Focus on dHvA quantum oscillations]

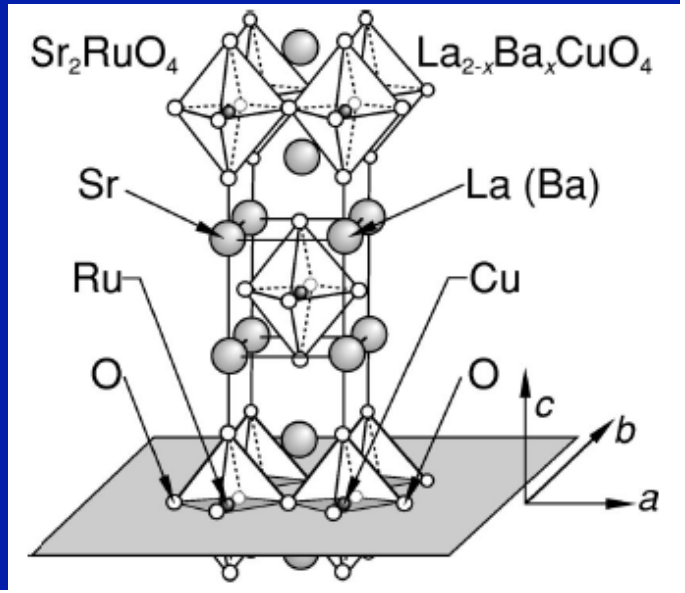

Yet, outstanding puzzles about this compound remain…

- A 4d material
  → expect not very large U (< 3eV)
- Yet, effective mass enhancement (vs. band/LDA value) as large as ~ 5
- Strong orbital dependence
- Low Fermi-liquid coherence scale:
- T^2 law obeyed only below ~ 30K
- Quasiparticles suppressed above ~ 130K, at which interlayer resistivity crosses over from metallic to insulating

Basic electronic structure :

- 4 electrons in t_{2g} shell
- d_{xy} orbital yields a quasi 2D band → γ-sheet of FS

- d_{xz}, (resp. d_{yz}) → bands with directional hopping along x (resp. y) → α,β sheets

Fermi surface of Sr_2RuO_4

and populations from dHvA:

FS from quantum oscillations:

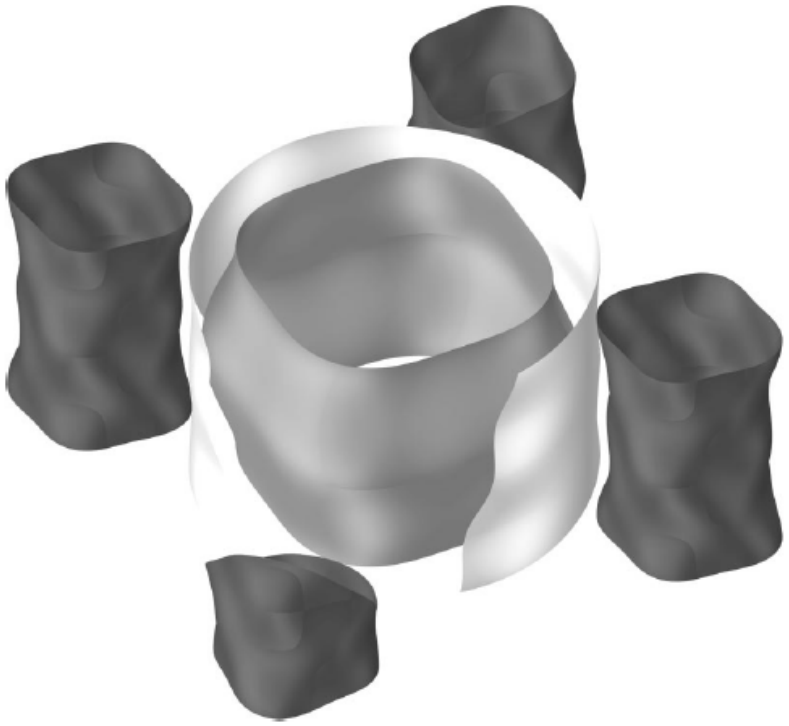

FS from photoemission:

β-sheet
(0.9 electrons)

α-sheet
0.2 hole

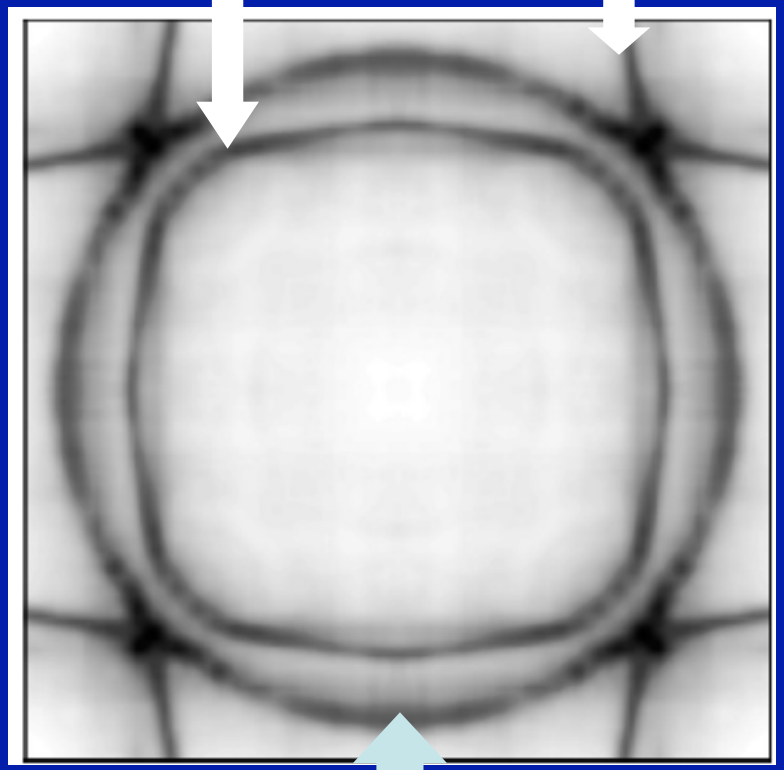

γ-sheet (xy)
1.3 electrons

Bands (LDA)

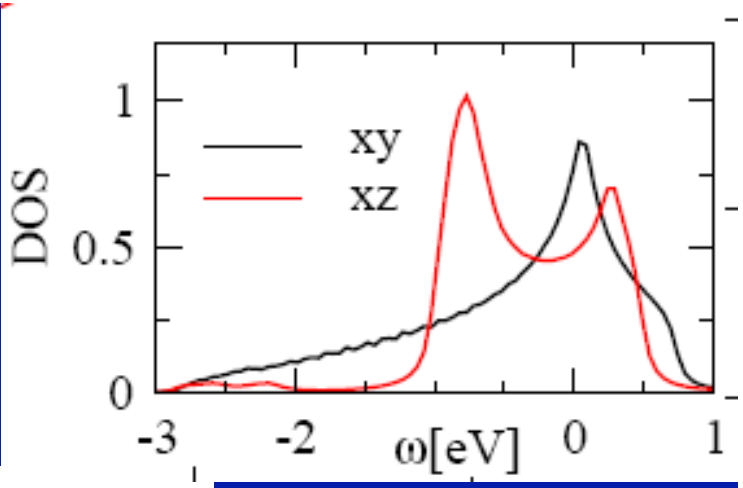

~ 1.5 eV
(xz,yz)

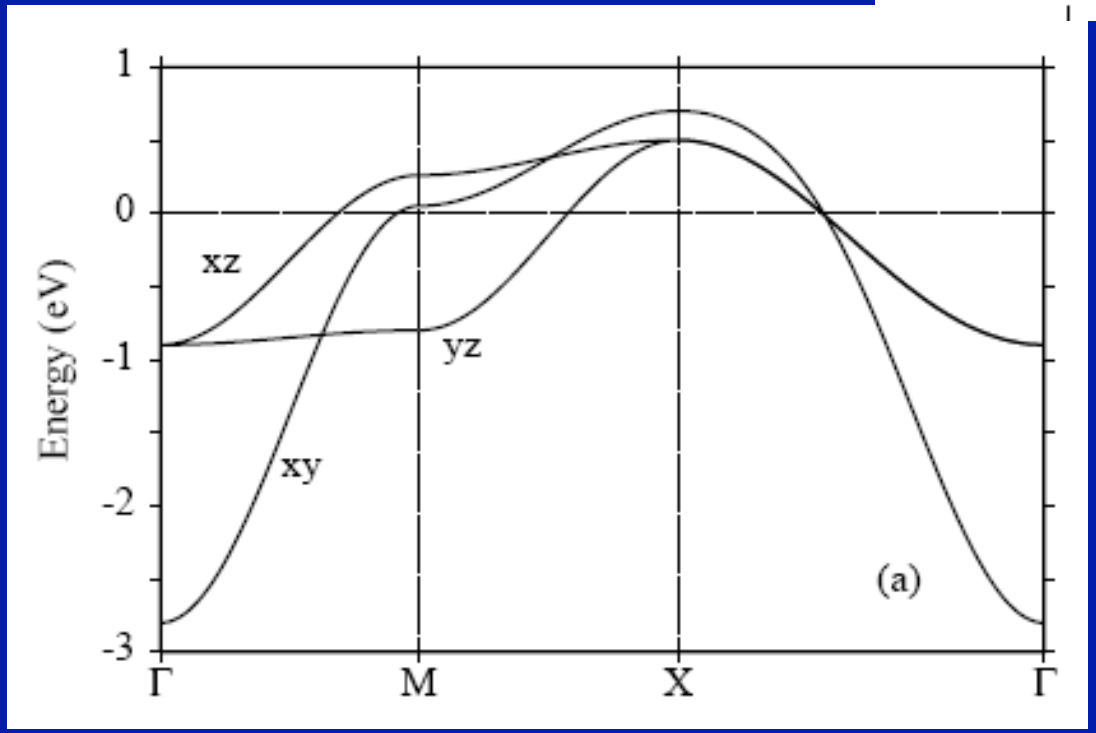

~ 3.6 eV
(xy band)

But kinetic energies of all bands comparable

Effective masses

TABLE II. Summary of quasiparticle parameters of Sr_2RuO_4.

Fermi-surface sheet	α	β	γ
Character	Holelike	Electronlike	Electronlike
k_F (Å^{-1})[a]	0.304	0.622	0.753
m^* (m_e)[b]	3.3	7.0	16.0
m^*/m_{band}[c]	3.0	3.5	5.5
v_F (ms^{-1})[d]	1.0×10^5	1.0×10^5	5.5×10^4
$\langle v_\perp^2\rangle$ (m^2 s^{-2})[e]	7.4×10^5	3.1×10^6	1.0×10^5
$t_\perp$ (K)[f]	7.3	15.0	2.7

-Rather large !

- Strongly orbital dependent.

- The widest band has the largest eff. mass enhancement !

Dynamical Mean-Field Theory calculations (using full LDA bandstructure):

- effective masses -

J [eV]	$m^*_{xy}/m_{\rm LDA}$	$m^*_{xz}/m_{\rm LDA}$	T^*_{xy}[K]	T^*_{xz}[K]	$T_>$[K]
0.0, 0.1	1.7	1.7	> 1000	> 1000	> 1000
0.2	2.3	2.0	300	800	> 1000
0.3	3.2	2.4	100	300	500
0.4	4.5	3.3	60	150	350

Table I. Mass enhancement of the xy and xz orbitals, as a function of Hund's coupling, for $U = 2.3$ eV. Other columns: coherence temperatures as defined in the text.

- Increase of effective mass as J is increased
- Orbital differentiation: xy heavier
- Comparable mass enhancement would require U=5eV at J=0 !

For U=2.3 eV

Contrast: Hund's correlations vs. Hubbard U
Sr_2RuO_4 (d^4) vs. $SrVO_3$ (d^1)

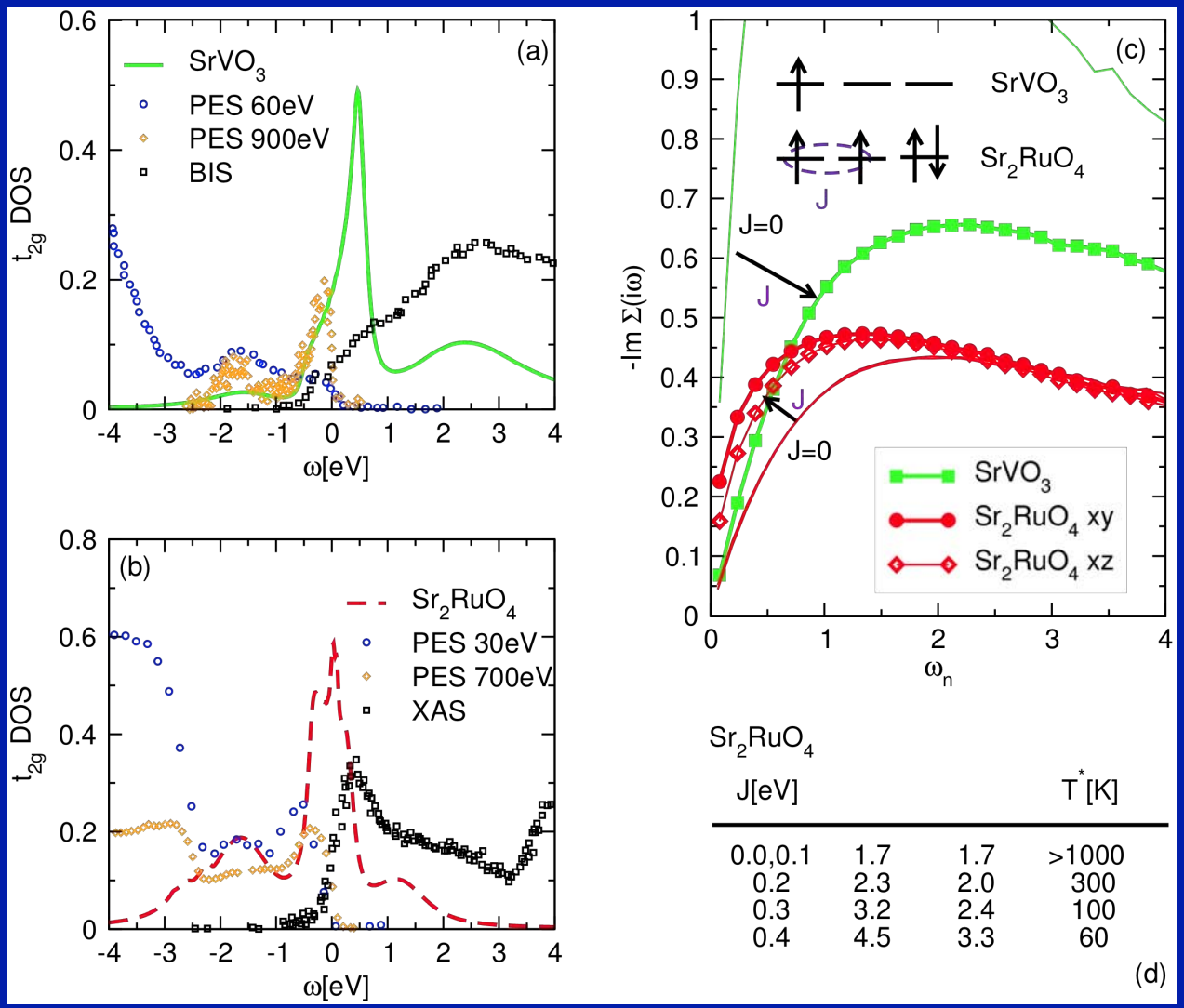

SrVO3:
Courtesy
M.Casula
Fig: J.Mravlje

Quasiparticle coherence scale

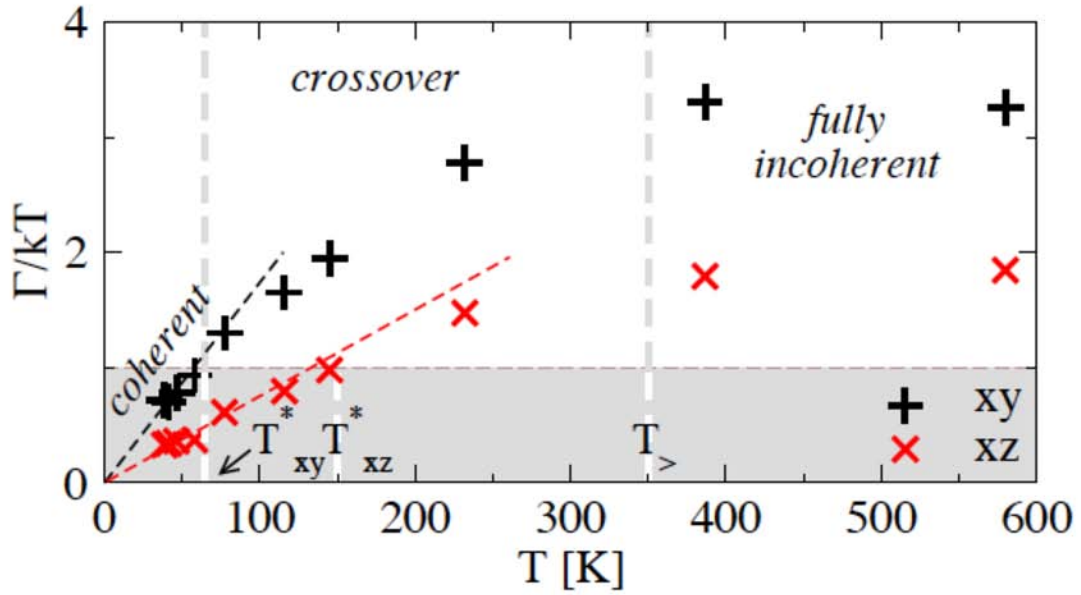

Figure 1. Temperature-dependence of Γ/kT, with $\hbar/\Gamma$ the quasiparticle lifetime. The shaded region corresponds to the 'coherent' regime with long-lived quasiparticles such that $\Gamma \lesssim kT$.

Inverse QP lifetime / T:

Fermi Liquid @ low-T
T-linear above ~ 400 K
Reaches ~kT at ~ 70K

Low-T calculations made possible by recent progress in DMFT technology: CT-QMC solver of P. Werner et al.

Comparison to ARPES

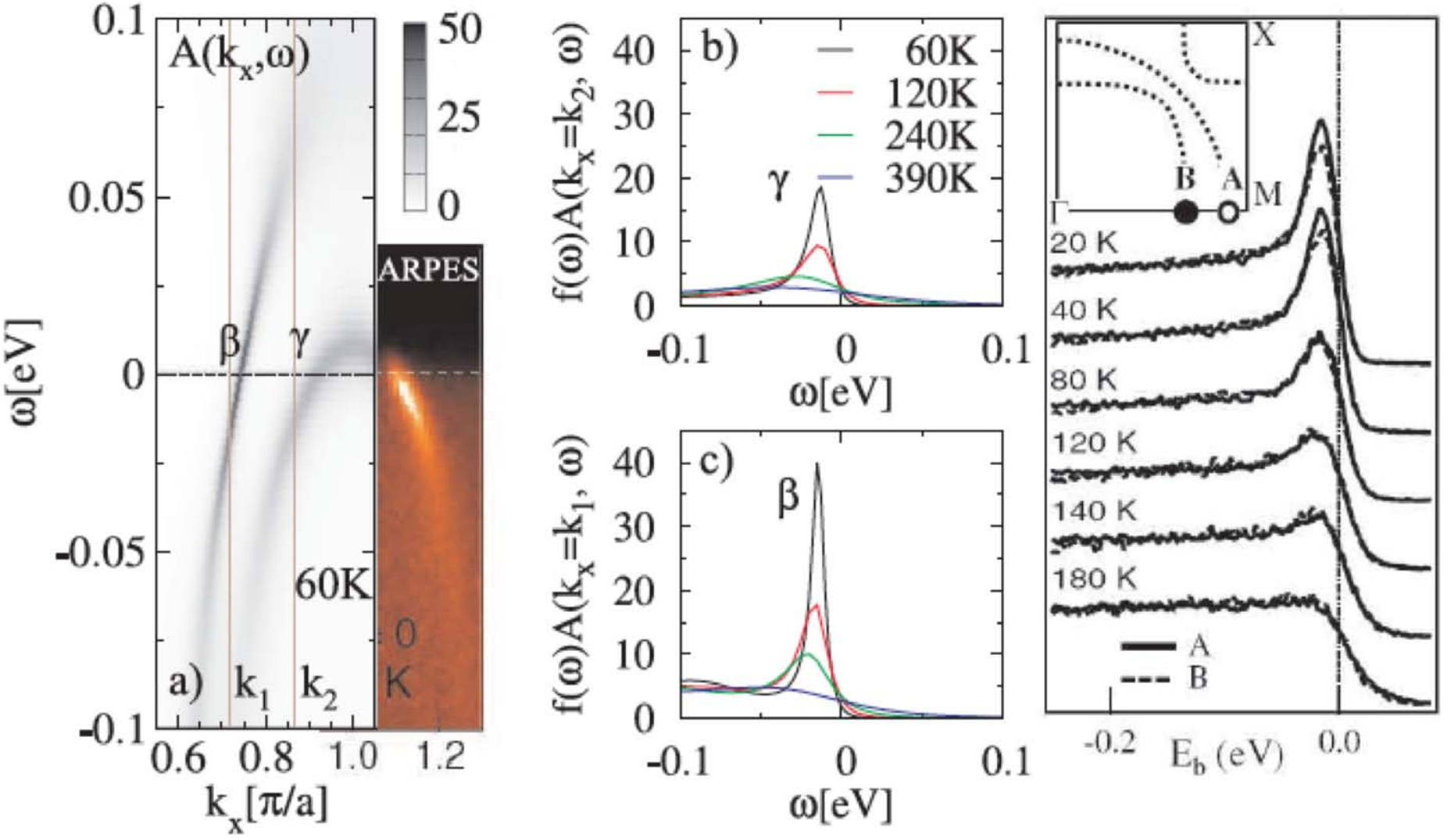

Figure 2. (a) Intensity map of the spectral function $A(k,\omega)$ along $\Gamma \rightarrow$M for $0.55\pi/a \leq k_x \leq 1.05\pi/a$, $k_y = 0$ at $T = 60$ K compared to ARPES [14]. (b,c) Spectral lineshapes at wavevectors k_1, k_2 compared to ARPES [3]. (d,e) $\mathrm{Im}\Sigma(\omega + \mathrm{i}0^+)$ and

Self-energies vs. ARPES

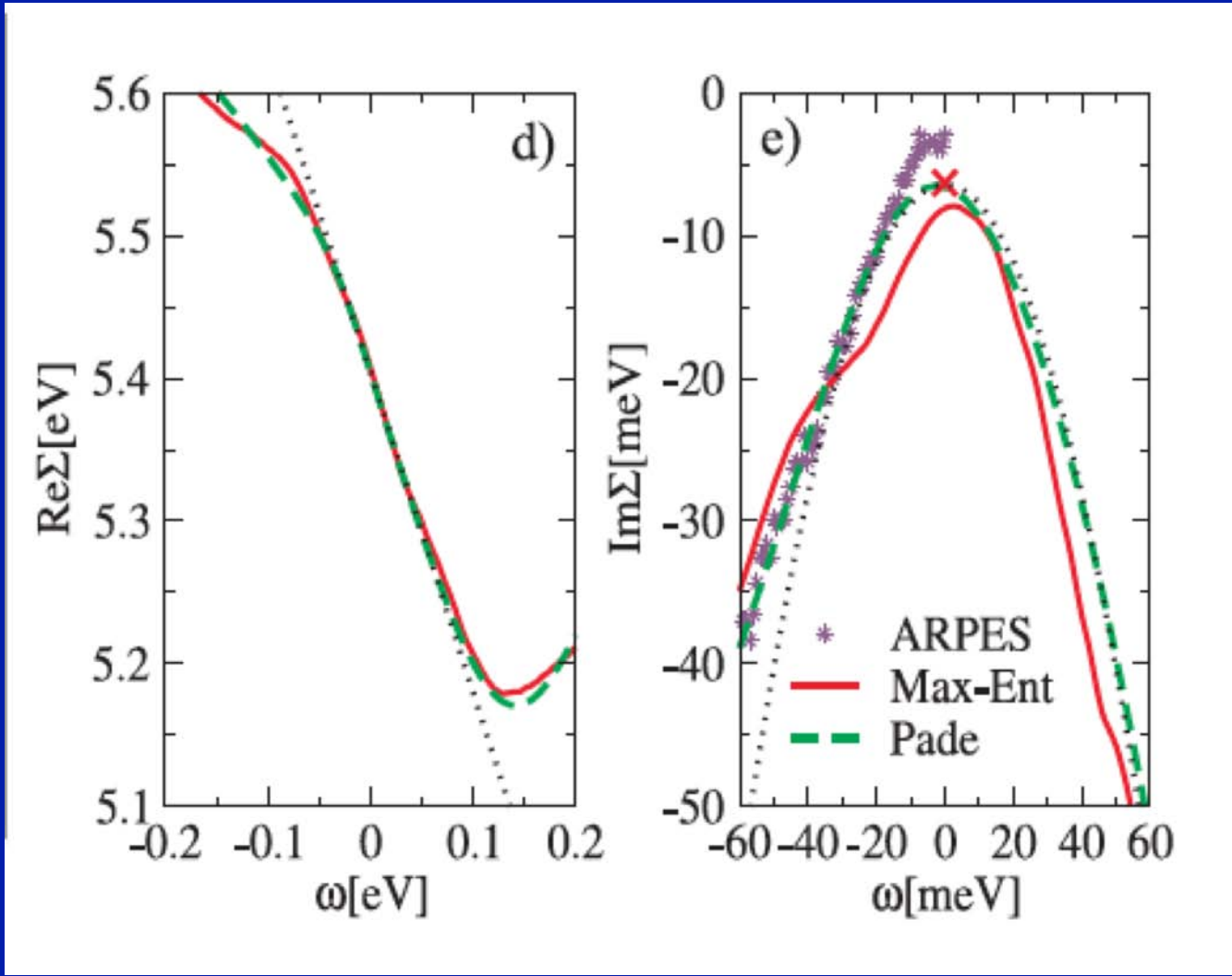

Orbital dependence: why is xy more correlated ?

Hund's coupling lowers the inter-orbital coupling:
Individual fermiology of orbitals becomes relevant

xy `effective hybridization strength' to environment is smaller (by at least a factor of 2) than xz, yz

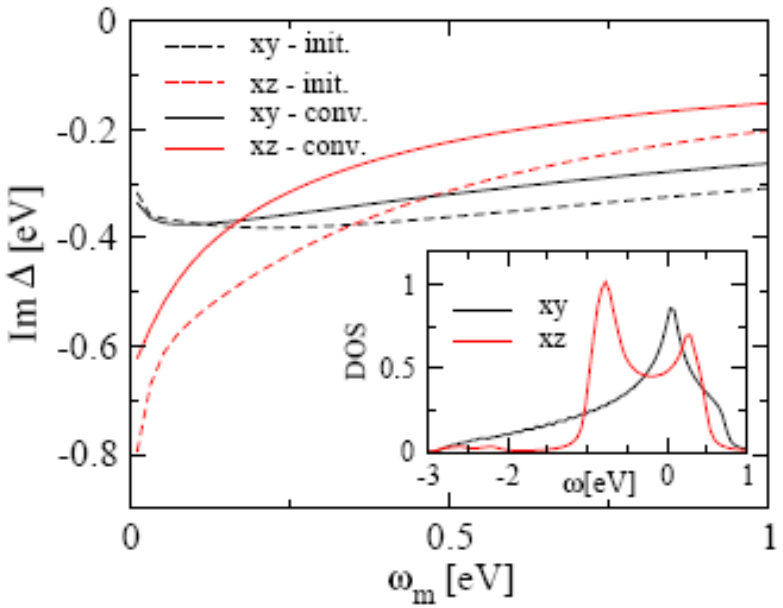

Initial LDA eff. Hybridization:

$$\mathrm{Im}\Delta(i\omega \to 0) = G_{\mathrm{loc}}^{-1} = -\frac{\mathrm{Im}G_{\mathrm{loc}}}{(\mathrm{Re}G_{\mathrm{loc}})^2 + (\mathrm{Im}G_{\mathrm{loc}})^2}.$$

Proximity of van Hove singularity for xy makes DOS larger and Strongly p-h asymmetric
→Both effects reduce hybridization

3. `Spin-freezing' regime and non Fermi-liquid behaviour

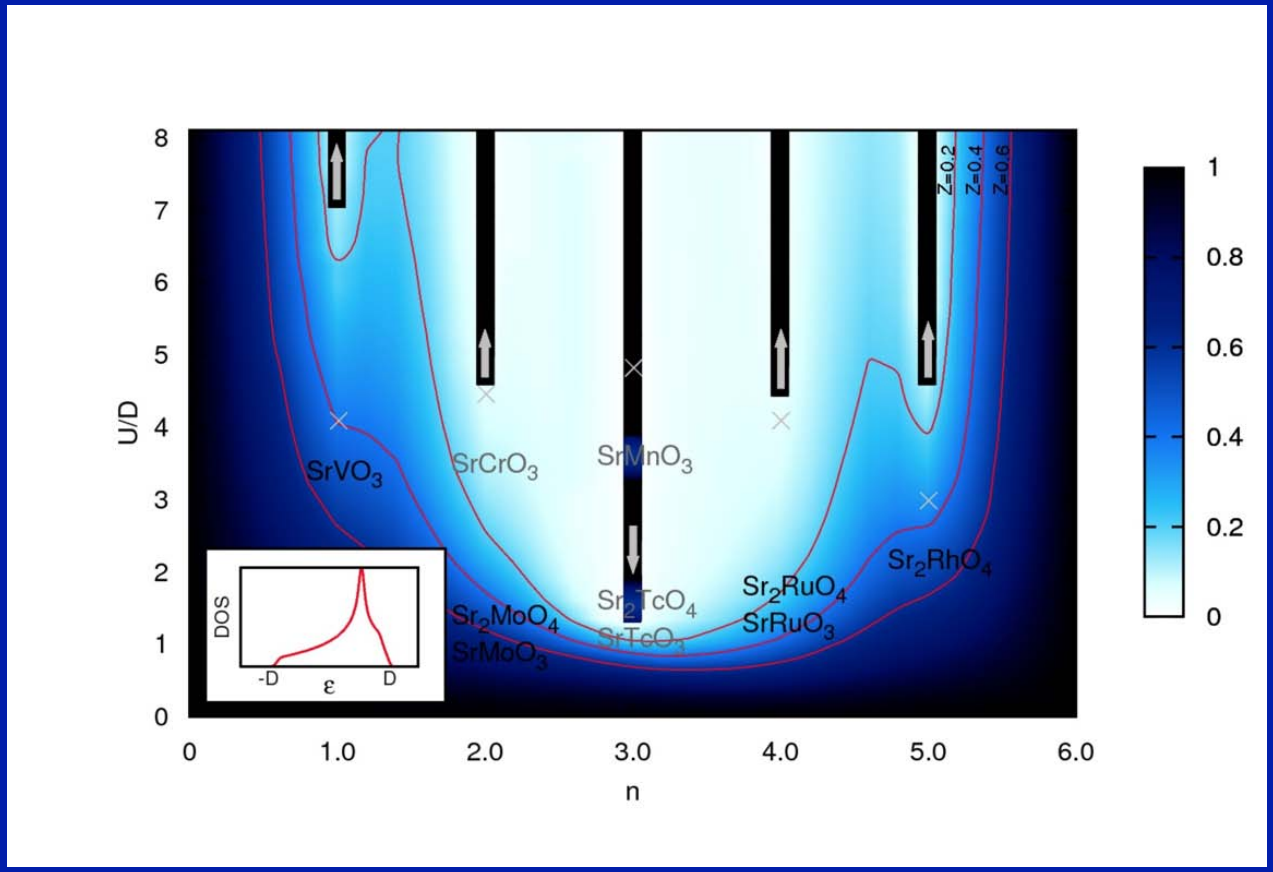

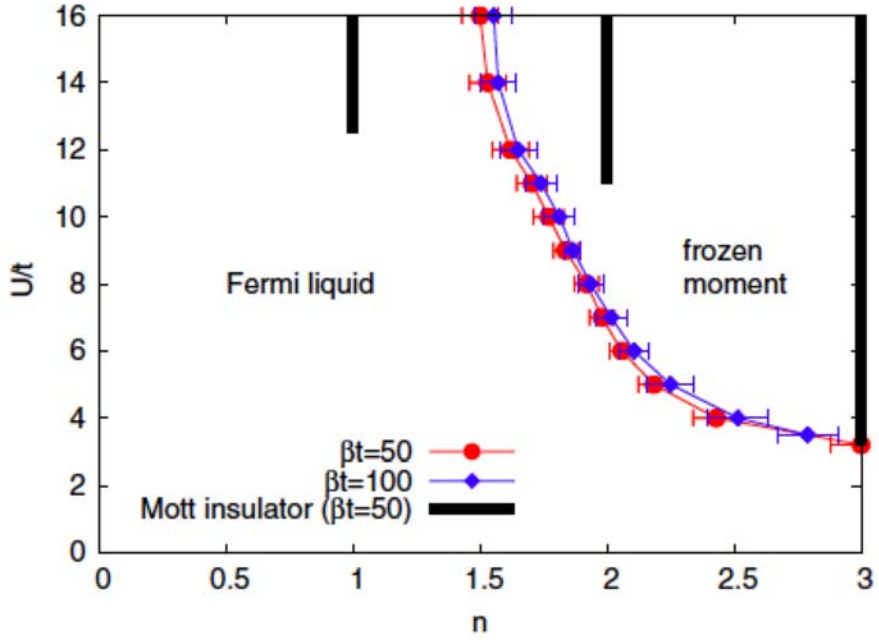

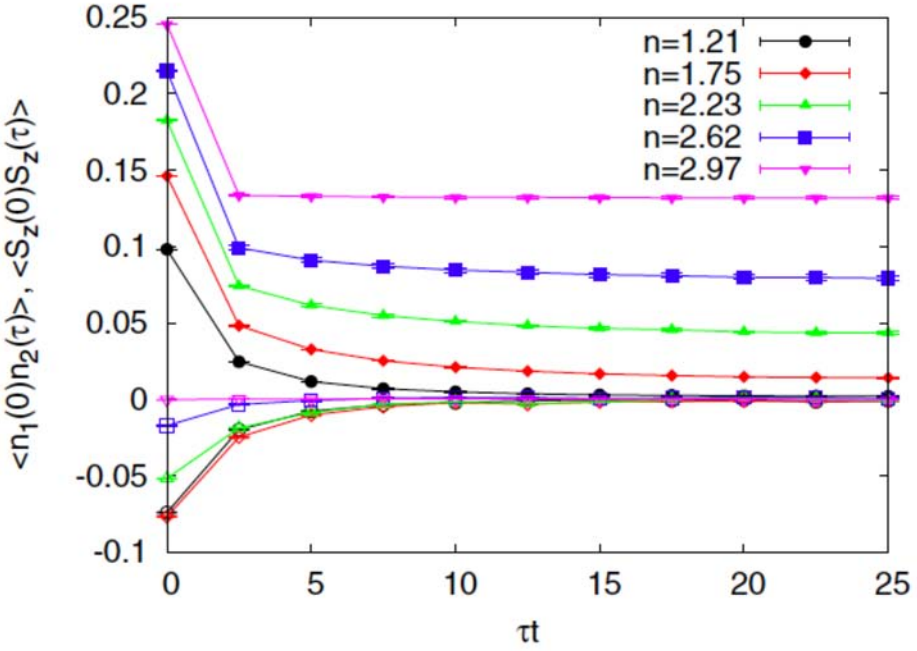

FIG. 1 (color online). Phase diagram for $J/U = 1/6$ and $\beta t = 50, 100$ in the space of density n and interaction strength U. The light line with circles or diamonds indicates a phase transition between a Fermi liquid metal and a "frozen-moment" metal. The black lines mark the regions of Mott insulating behavior.

`Spin freezing'
Werner et al. PRL 2008
Haule&Kotliar NJP 2009

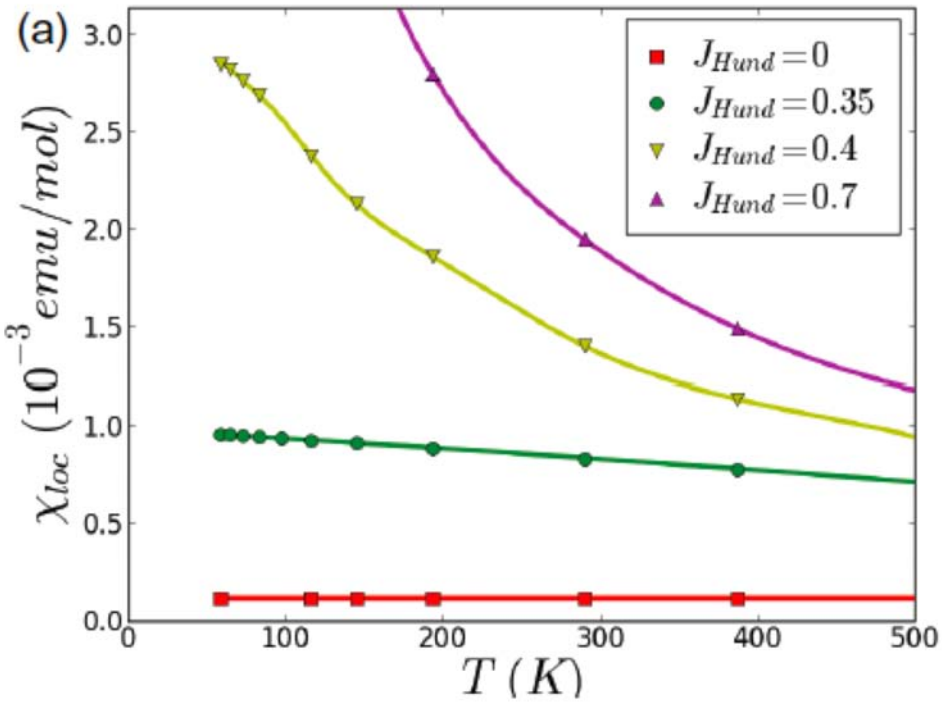

Non Fermi-Liquid regime
Power-law self-energy
(P.Werner et al)

$$D\, Im\Sigma \sim C + (\omega/D)^{\alpha}$$

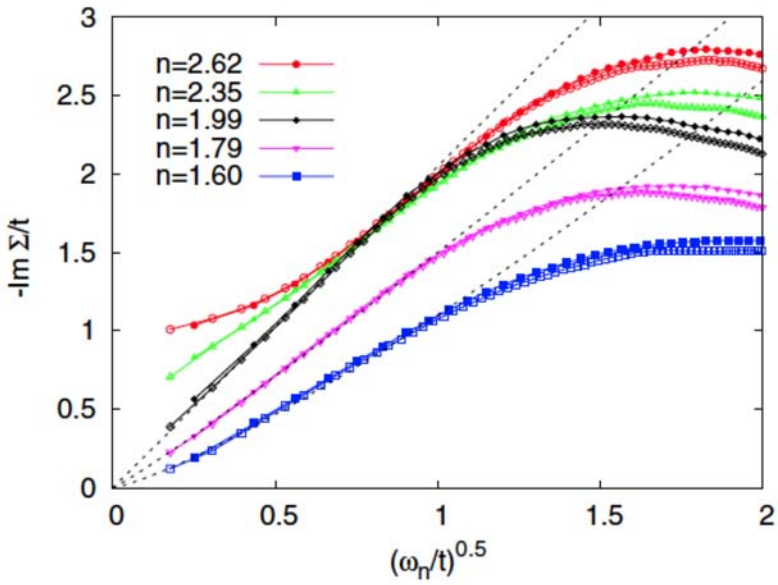

FIG. 3 (color online). Doping dependence of the imaginary part of the Matsubara axis self-energy for $U/t = 8$, $\beta t = 50$ (full symbols) and 100 (open symbols) at dopings indicated. The dashed lines are proportional to $(\omega_n/t)^{\alpha}$, $\alpha = 0.5, 0.54, 0.62$ (from top to bottom).

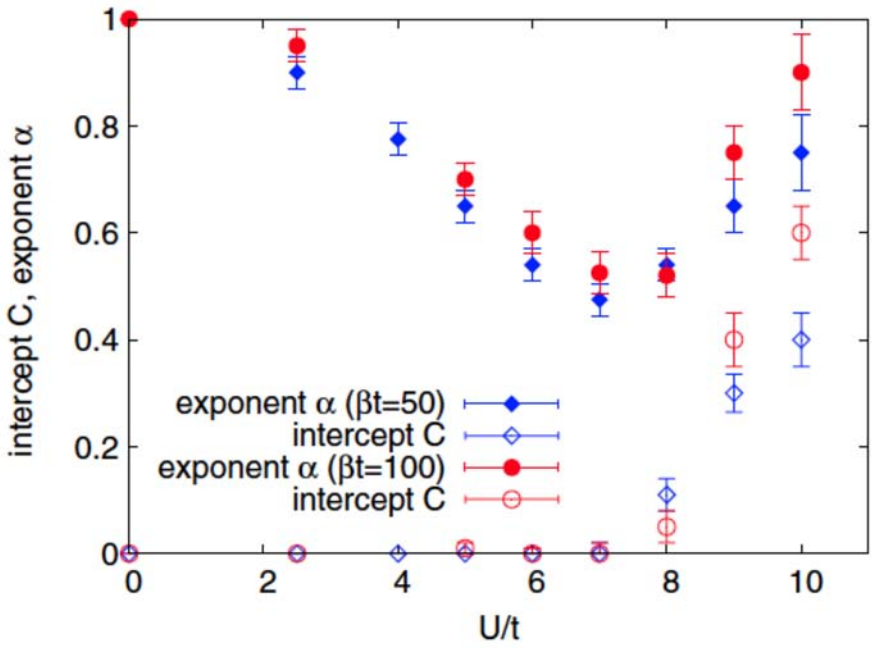

FIG. 4 (color online). Results of a fit of the computed Matsubara-axis self-energy to the scaling form $-\mathrm{Im}\Sigma/t = C + A(\omega_n/t)^{\alpha}$ at temperatures $T = t/50$ (diamonds; blue online) and $T = t/100$ (circles; red online) at density $n = 2$ and interaction strengths indicated. The plot illustrates the wide quantum critical regime of the spin-freezing transition.

A Fermi liquid is recovered at (very) low T

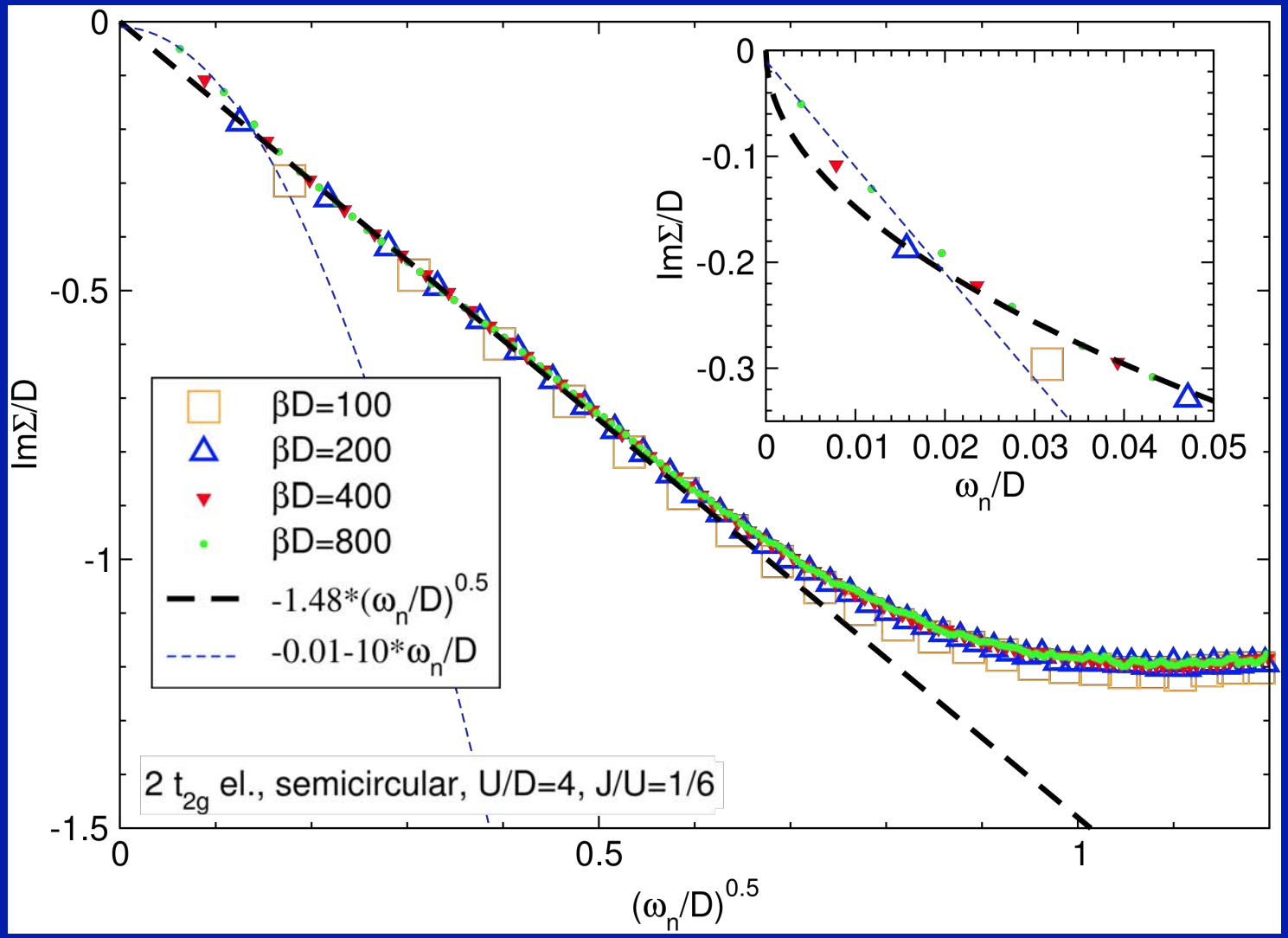

Courtesy J.Mravlje

Possible phenomenological consequences

Theory still partly to be worked out
and experimental evidence wanted !

Bad metal, non-T^2 resistivity ($T^{1/2}$?)
Non-Drude optics at low-frequency ($1/\omega^{1/2}$?)
Local moments coexisting with metallic transport

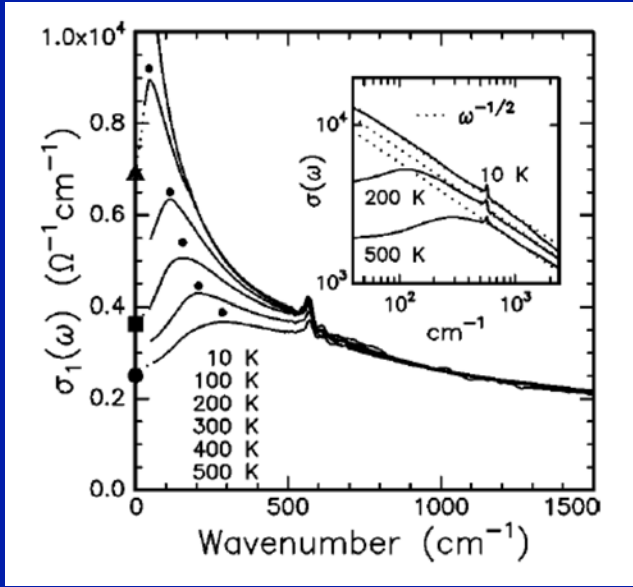

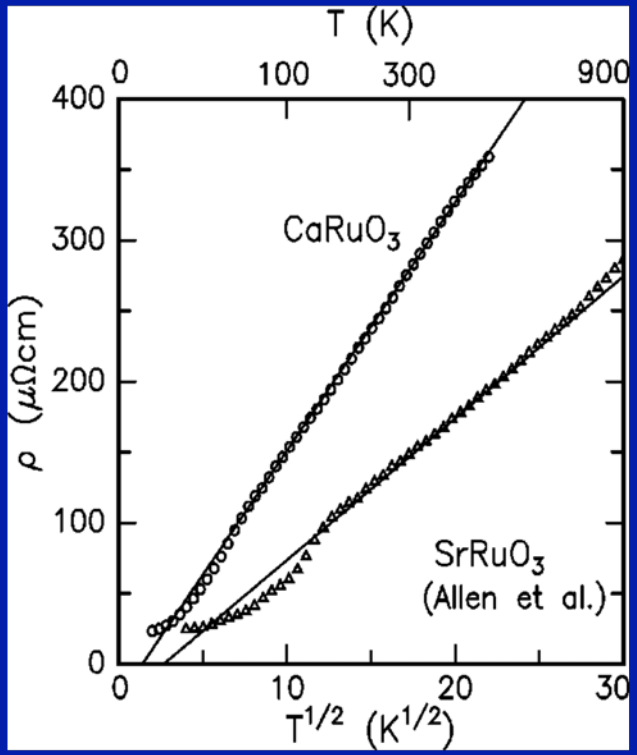

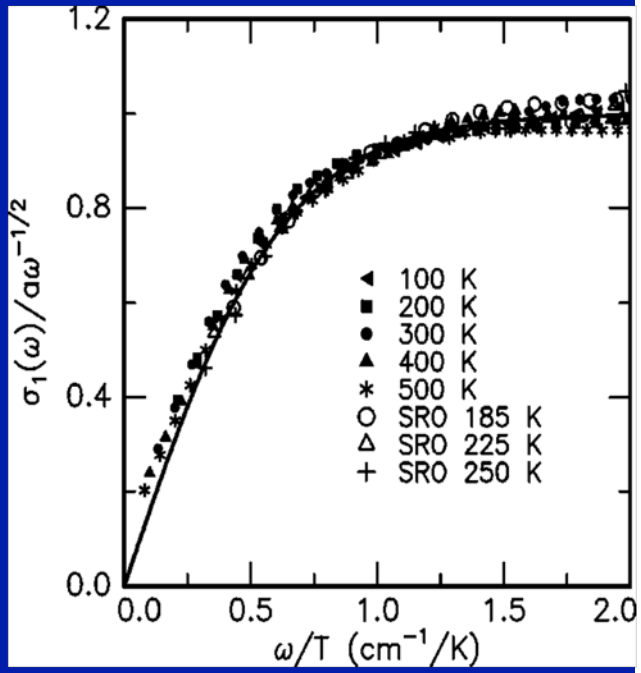

Lee et al.
PRB 66 041104 (2002)

4. Current status of theoretical understanding → Blackboard

Key ref: L. De Leo PhD thesis (SISSA, Trieste)
See also: De Leo and Fabrizio, PRB 69 (2004) 245114

After Schrieffer-Wolf transformation of impurity model:

Strategy
(a la Nozieres-Blandin)
Diagonalize HK first
Residual degree of freedom and interaction ?

$$
\begin{aligned}
H_K &= -J\left[2\vec{S}_d\cdot\vec{S}_d+\frac{1}{2}\vec{T}_d\cdot\vec{T}_d\right] \\
&\quad +\frac{4t^2}{U}\sum_{ab}\sum_{\alpha\beta}c^\dagger_{1,a\alpha}c_{1,b\beta}d^\dagger_{b\beta}d_{a\alpha} \\
&\quad -\frac{2t^2}{U}\sum_{a\alpha}\left(c^\dagger_{1,a\alpha}c_{1,a\alpha}+d^\dagger_{a\alpha}d_{a\alpha}\right)
\end{aligned}
$$

$$
\begin{aligned}
H &= H_K+H_{cond} \\
&= H_K+\sum_{n=1}^{\infty}t_n\left(c^\dagger_{n,a\alpha}c_{n+1,a\alpha}+h.c.\right).
\end{aligned}
$$

Spectrum of atomic t_{2g} hamiltonian with U'=U-2J

N	S	L	Degeneracy $= (2S+1)(2L+1)$	Energy
0,[6]	0	0	**1**	0
1,[5]	1/2	1	**6**	$-5J/2$,$[10\mathcal{U}-5J/2]$
2,[4]	1	1	**9**	$\mathcal{U}-5J$,$[6\mathcal{U}-5J]$
2,[4]	0	2	5	$\mathcal{U}-3J$,$[6\mathcal{U}-3J]$
2,[4]	0	0	1	$\mathcal{U}$,$[6\mathcal{U}]$
3	3/2	0	**4**	$3\mathcal{U}-15J/2$
3	1/2	2	10	$3\mathcal{U}-9J/2$
3	1/2	1	6	$3\mathcal{U}-5J/2$

Table 1: Eigenstates and eigenvalues of the t_{2g} Hamiltonian $\mathcal{U}\hat{N}(\hat{N}-1)/2 - 2J\vec{S}^2 - J\vec{T}^2/2$ in the atomic limit ($\mathcal{U} \equiv U - 3J$). The boxed numbers identifies the ground-state multiplet and its degeneracy, for $J > 0$.

- Hund's rule ground-state in each particle-number sector
- Symmetry broken by J from SU(6) to U(1)c×SU(2)s×SO(3)o
- → Degeneracies lifted by J

Iron-based superconductors: pnictides and chalcogenides

A controversial question since discovery (2008):
How correlated are these materials ?

- Weak coupling itinerant antiferromagnets (SDW)
  a.k.a Chromium ?

- Strongly correlated metals, possibly driven
  by Hund's coupling rather than proximity to Mott ?

- Very localized magnetism